Identification of zeotropic mixtures of natural refrigerants for enhanced performance in geothermal district heating heat pumps

Virginia Natonek [a], Jonas Kjær Jensen [a], Wiebke Brix Markussen [b*]

[a] Technical University of Denmark, Koppels Allé, 2800 Kgs. Lyngby, Denmark
[b] Danish Technological Institute, Gregersensvej, 2630 Taastrup, Denmark

Abstract

Decarbonizing district heating supply is essential for achieving climate targets, and heat pumps utilizing renewable geothermal energy represent a viable technology option for this. Conventional heat pumps typically employ pure or azeotropic refrigerants, which, under the large sink and source temperature variations characteristic of geothermal district heating, can result in poor temperature matching and increased irreversibilities, thereby limiting system efficiency. These irreversibilities can be mitigated by operating several heat pumps in series, subsequently complicating the system design; thus, a solution using a single heat pump is preferable. Using zeotropic mixtures in a single-stage heat pump is an option for achieving high efficiency with a simple system design. This study aims to numerically investigate possible performance improvements of heat pumps in geothermal district heating applications by systematically optimizing the mixture components and the composition of the applied zeotropic mixture. All investigated mixtures were blends of hydrocarbons, and the optimization objective was to maximize the yearly average efficiency across five representative operating conditions. A detailed numerical model, implemented in Python and using the REFPROP for thermophysical property calculations, was applied to simulate a single-stage heat pump cycle with an internal heat exchanger. Results indicate that the optimized zeotropic mixtures provide improved alignment with varying heat source and sink temperatures, yielding an increase in annual average coefficient of performance (COP) compared to the best-performing pure fluid. These findings underscore the potential of natural zeotropic refrigerant mixtures to significantly improve the efficiency of geothermal-based district heating systems across different operating conditions.

Keywords: Mixture refrigerants; zeotropic mixtures; hydrocarbons; geothermal heat pumps

1. Introduction

Europe is experiencing a significant push toward decarbonizing its heating sector, with space heating and industrial heating accounting for a large share of final energy use. In this sector, heat pumps are gaining increasing attention as an efficient and low-emission alternative to conventional fossil-based systems [1]. However, traditional heat pump systems typically rely on pure fluids or azeotropic mixtures as working fluids. These refrigerants evaporate and condense at constant temperatures, which can lead to poor temperature matching with the heat source and the heat sink. This mismatch causes increased irreversibilities during heat transfer, limiting the overall system performance [2]. To address this inefficiency, zeotropic refrigerant mixtures have been proposed as a promising alternative [3]. Zeotropic mixtures consist of two or more components with different properties. During liquid-vapour phase change, the mixture composition of the

* Corresponding author. Tel.: +45 7220 2179
E-mail address: wbm@teknologisk.dk

15th IEA Heat Pump Conference 2026 - REF1.2 - https://doi.org/10.23697/m83q-sm64

liquid and vapour changes, resulting in a changing boiling point and vapour pressure throughout the phase change process. Consequently, the mixture changes phase over a range of temperatures. This temperature range is called the temperature glide [4]. The temperature glide hence allows better alignment with the temperature profiles of the heat source and heat sink, reducing exergy destruction and potentially increasing the coefficient of performance (COP) [2], [4]. To fully realize the advantages of zeotropic mixtures in heat pump design, systematic screening methods are needed to identify mixtures that match the heat source/sink profiles and meet the required performance criteria.

Zühlsdorf et al. [5] consider 18 pure fluids and all possible binary combinations of these for booster heat pumps in district heating networks. The district heating forward temperature was 40 °C, and the booster heat pump was used to produce domestic hot water at 60 °C. The study shows that mixing pure fluids allows an improvement of 47 % in COP compared to R-134a. In particular, mixtures of (50 % propylene – 50 % butane) and (50 % R1234yf – 50 % R1233zd(E)) achieve superior thermodynamic performance compared to pure fluids.

Abedini et al. [6] explore the use of zeotropic refrigerant mixtures for high-temperature heat pumps (HTHP) operating in the range between 100 ˚C and 200 ˚C. Three industrial processes with different heat sources and sinks are examined: a distillation process (latent-to-latent heat transfer), superheated steam drying (latent-to-sensible), and a pressurized water production process (sensible-to-sensible). The first two cases demonstrate the key benefits of zeotropic mixtures over pure fluids, particularly in terms of reduced compression ratio and lower compressor outlet temperature, while the latter case shows an increase in COP by 10 % using binary zeotropic mixtures, especially with hydrocarbons.

Moreover, Zühlsdorf et al. [7] study a set of six refrigerants and all their possible binary combinations for applications in the context of spray drying processes in the dairy industry, with heat sink temperature reaching 130 ˚C. Their analysis shows that the top performing mixtures in terms of COP are (50 % propane – 50 % isobutane), (90 % n-butane – 10 % n-hexane), and (60 % n-butane – 40 % n-pentane), which all achieve a COP of 3.08, whereas the best-performing pure components are n-butane, isobutane and isopentane, with COP equal to 2.89, 2.78 and 2.78, respectively. Therefore, using a zeotropic mixture demonstrates an improvement of 6.6 % in terms of COP.

Guo et al. [8] study potential zeotropic hydrocarbon mixtures as alternative working fluids in a HTHP heating water from 15˚ C to 99 ˚C. They use a performance analysis and optimization algorithm to investigate five binary zeotropic mixtures. The study concludes that the mixtures (n-hexane - propene) and (R4310mee - R32) achieve higher COP and improve exergy utilization due to a better match of the heat sink with the refrigerant.

Lastly, Agrawal et al. [9] conduct an experimental assessment comparing the performance of a domestic refrigerator using a mixture of (50 % propane – 50 % iso-butane) with R-134a under different charge conditions. The results demonstrate that the mixture exhibits a higher COP in all operating conditions tested.

Overall, the reviewed literature confirms that zeotropic mixtures can significantly enhance heat pump performance when tailored to specific boundary conditions, primarily through improved temperature matching and reduced pressure ratios.

However, existing research focuses on identifying optimal mixtures for single, fixed boundary conditions, while this study takes the identification a step further by determining the best performing mixtures over a range of operating conditions. To address this gap, we present a systematic and scalable screening framework capable of evaluating and comparing zeotropic mixtures across multiple operating scenarios. The framework applies a three-stage approach to progressively filter and identify mixtures that combine high thermodynamic performance with robustness under various boundary conditions. The framework was applied to a case study focusing on heat pumps for geothermal district heating.

2. Methodology

This chapter describes the methodological framework combining numerical modelling and multi-stage screening to identify zeotropic mixtures capable of improving heat pump performance under diverse operating conditions. The procedure involves generating a refrigerant mixture database, simulating the thermodynamic cycle, and iteratively refining mixture selection through performance, technical feasibility, and robustness criteria.

2.1. Thermodynamic model

A steady-state numerical model was developed to simulate a single-stage heat pump cycle with an internal heat exchanger (IHX), allowing for both subcritical and transcritical operation modes. The choice is justified by the modest temperature lift between heat source and heat sink, and the desire for a simple cycle layout. The cycle follows the layout of Zühlsdorf et al. [10] comprising an evaporator that absorbs heat from the geothermal water circuit, a compressor with fixed isentropic efficiency (see Table 1), a condenser that transfers heat to the district heating network, modelled as three zones (de-superheating, condensation, and subcooling), and an expansion valve, treated as an isenthalpic device (see Figure 1).

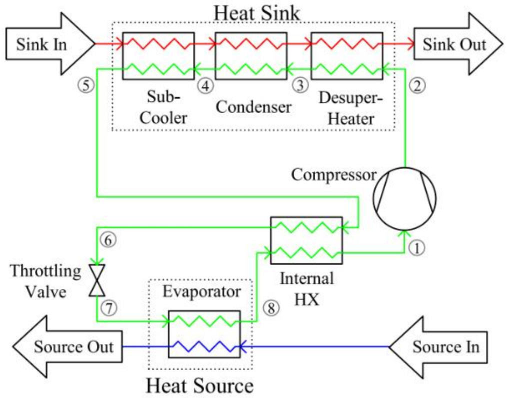

Figure 1. Layout of the heat pump cycle [10].

The energy balance across each component was expressed as:

$$\dot{Q} + \dot{W} = \dot{m}(h_{\text{in}} - h_{\text{out}}) \quad (1)$$

The cycle performance was quantified by:

$$\text{COP} = \frac{\dot{Q}_{\text{sink}}}{\dot{W}_{\text{comp}}} \quad (2)$$

In addition, the volumetric heating capacity (VHC) was used as an indicator of the compressor size. It relates the supplied heat $\dot{Q}_{\text{sink}}$ to the volume flow rate at the inlet of the compressor $\dot{V}_1$.

$$\text{VHC} = \frac{\dot{Q}_{\text{sink}}}{\dot{V}_1} \quad (3)$$

Pinch-point constraints of 3 K were enforced for all heat exchangers. Pressure drops were distributed across discretized segments (20-30 nodes per heat exchanger). Pressure levels were initialized based on critical properties and adjusted via a root-finding solver to satisfy the pinch point constraints simultaneously at source and sink sides. The model outputs included COP, pressures, and temperature profiles.

The present model is based on the model developed by Zühlsdorf et al. [11]. It was implemented in Python [12] using REFPROP v10.0 [13] for refrigerant properties and CoolProp [14] for water circuits. The model was validated against data from Zühlsdorf et al. [10] and Vieren et al. [15] for both pure fluids and zeotropic mixtures.

2.2. Application to case studies

The proposed operating scenarios were provided by a Danish geothermal facility supplying heat to the district heating network in the city of Aarhus, Denmark. A total of five cases were identified, each associated with different temperature profiles at the sink (district heating water circuit) and source (geothermal water circuit), as well as the annual operating hours. The identified case scenarios reflect the requirements imposed by the local district heating company. Table 2 summarizes the temperature pairs for the selected operating cases. Case III exhibits the smallest temperature lift, suggesting more favourable thermodynamic conditions and the potential for a higher COP. In contrast, cases with larger temperature lifts are expected to operate with lower efficiencies.

Table 1: Summary of thermodynamic, discretization, and performance parameters defining the boundary conditions and component settings of the simulated heat pump cycle.

Definition	Parameter	Value	Unit
Minimum superheat at evaporator outlet	ΔT_{sh}	0	K
Minimum pinch temperature at source HX	$\Delta T_{pinch, source}$	3	K
Minimum pinch temperature at sink HX	$\Delta T_{pinch, sink}$	3	K
Minimum pinch temperature at IHX	$\Delta T_{pinch, IHX}$	3	K
Discretization points in the evaporator	n_{evap}	20	–
Discretization points in the superheater	n_{sh}	4	–
Discretization points in the desuperheater	n_{desup}	5	–
Discretization points in the condenser	n_{cond}	20	–
Discretization points in the subcooler	n_{sc}	5	–
Compressor isentropic efficiency	η_{is}	75	%
Motor efficiency	η_{mech}	95	%
Compressor heat loss factor	f	0	–
Source heat load	$\dot{Q}_{source}$	500,000	W

Table 2. Cases for the geothermal operation.

	Load hours (hrs)	$T_{source, in}$ (˚C)	$T_{source,out}$ (˚C)	$T_{sink,in}$ (˚C)	$T_{sink,out}$ (˚C)
Case I	2000	40	7	50	80
Case II	1250	40	7	55	85
Case III	1000	45	20	45	70
Case IV	750	40	7	55	90
Case V	500	45	25	60	90

2.3. List of refrigerants

The list of refrigerants was obtained from a previous study carried out by Zühlsdorf et al. [9], in which the fluids were selected based on their thermodynamic properties, miscibility, and environmental and safety factors. The list comprises natural refrigerants, ethers, hydrofluoroolefins (HFOs), and hydrochlorofluoroolefins (HCFOs). The refrigerants are selected based on characteristics such as low global warming potential (GWP), zero ozone depleting potential (ODP), and low flammability. However, for this study, only hydrocarbons (HC) mixtures were investigated, reducing the list to the 10 refrigerants, described in Table 3.

Table 3. List of fluids considered in the screening with characteristic properties

No.	Name of Fluid	Ref. No.:	ODP (-)	GWP (-)	T_{boil} (°C)	T_{crit} (°C)	p_{crit} (bar)	Safety Class
1	ethane	R-170	0	6	-88.6	32.2	48.7	A3
2	ethylene	R-1150	0	4	-103.8	9.2	50.4	A3
3	propane	R-290	0	3	-42.0	96.7	42.5	A3
4	propylene	R-1270	0	2	-47.6	91.1	46.7	A3
5	iso-butane	R-600a	0	3	−11.7	134.7	36.3	A3
6	n-butane	R-600	0	3	-0.5	152.0	38.0	A3
7	iso-pentane	R-601a	0	4	27.8	187.3	33.8	A3
8	pentane	R-601	0	4	36.1	196.6	33.3	A3
9	n-hexane				68.7	234.5	30.3	A3
10	Heptane				98.4	267.0	27.4	A3

2.4. Screening Framework

A systematic screening was implemented to evaluate mixtures based on energetic and exergetic performance indicators, as well as typical technical constraints. The framework consists of three sequential stages: Exploratory, Refinement, and Validation, each filtering the mixtures based on different criteria. Figure 2 illustrates the step-wise screening process.

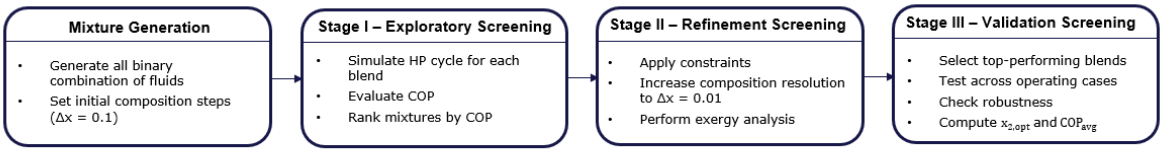

Figure 2. Flowchart of the three-stage screening framework used for refrigerant mixture selection and evaluation.

2.4.1. Stage I – Exploratory Screening

The first stage of the screening aimed at simulating all the possible binary combinations of the selected refrigerants present in Table 3. The mixtures were generated with composition steps of $\Delta x = 0.1$, and the heat pump cycle model was run for each composition. In this stage, the COP was used as a key metric to identify promising candidates.

2.4.2. Stage II – Refinement Screening

In the second stage of the screening, engineering constraints were introduced. Namely, the allowed pressure levels were in the range of 2 bar to 20 bar and the maximum allowed temperature at the discharge line of the compressor was set to 140 ˚C. Mixtures violating these constraints were excluded from further consideration. For this refined set, exergy analysis was performed after increasing the composition resolution of blends from 10 % to 1 %, thus allowing more precise identification of optimal compositions. The approach used follows the methodology proposed by Zühlsdorf et al. [16], who investigated the performance of mixtures in relation to the sink and source during phase change. For this, the concept of glide matching indicators, π_{glide}, was proposed by Zühlsdorf et al. [16]. These indicators assess the degree of alignment between the temperature profiles of the blend and sink/source streams. It is expressed as follows:

$$\pi_{\text{glide}} = \frac{\dot{E}_{D,\text{component}}}{\dot{E}_{D,\text{pinch}}} = \frac{\dot{E}_{D,\text{fluid}} + \dot{E}_{D,\text{pinch}}}{\dot{E}_{D,\text{pinch}}} \quad (4)$$

Where $\dot{E}_{D,\text{pinch}}$ is the exergy destruction associated with the component having finite heat exchange area, and it is defined as:

$$\dot{E}_{D,\text{pinch}} = T_0 \dot{Q} \left(\frac{\bar{T}_{\text{hot}} - \bar{T}_{\text{cold}}}{\bar{T}_{\text{hot}} \cdot \bar{T}_{\text{cold}}} \right) \quad (5)$$

In Eq. ((4), $\dot{E}_{D,\text{fluid}}$ represents the exergy destruction due to the non-ideality of the refrigerants, and it is obtained from $\dot{E}_{D,\text{component}}$, which refers to the rate of exergy destruction within a component, and it is generally described as:

$$\dot{E}_{D,i} = \dot{E}_{f,i} - \dot{E}_{p,i} \quad (6)$$

Where $\dot{E}_{f,i}$ is the exergy consumed to drive the component, while $\dot{E}_{p,i}$ is the useful exergy delivered by the component [17]. Using Eq. (4, a perfect temperature profile match corresponds to $\pi_{\text{glide}} = 1$, indicating that all exergy destruction is due solely to the finite temperature difference and cannot be further reduced by selecting a better-matched working fluid. Higher values of glide indicate increasing mismatch, and consequently a larger share of avoidable exergy destruction from poor temperature alignment between the working fluid and the external stream [16].

A schematic representation of this concept is shown in Figure 3, where the temperature-heat diagram highlights how mismatches between the mixture glide and the external stream profiles contribute to avoidable exergy destruction [16].

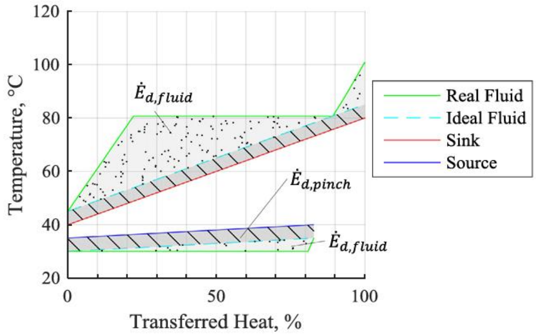

Figure 3. Diagram with temperature profiles over transferred heat with exergy destruction highlighted [16]

2.4.3. Stage III – Validation Screening

The mixtures selected from the previous stage were tested across all five cases. A weighted average COP_{avg} was calculated based on the operational hours and performance in each of the five cases:

$$\mathrm{COP}_{\mathrm{avg}} = \frac{\sum_{i=1}^{n}(\mathrm{COP}_i \cdot t_i)}{\sum_{i=1}^{n} t_i} \tag{7}$$

Here, COP_i was the COP achieved by a mixture in case i and t_i was the number of operating hours of case *i*, and *n* was the number of cases. To ensure robustness under various operating conditions, an additional selection criterion was introduced to determine the optimal composition among the top-performing mixtures. Specifically, a composition was considered optimal only if it returned valid results across all five cases, resulting in neither convergence issues nor violations of the engineering constraints. Additionally, the selected composition must have tolerated ±5 % variations in component fractions while still producing valid simulation outcomes. The resulting change in COP within this range was then evaluated to assess performance sensitivity, ensuring that the final selections remain both efficient and resilient to minor deviations from the optimal mixture composition.

3. Results

This section presents the results obtained from the screening procedure for both scenarios, outlining the step-by-step process leading to the identification of the optimal mixtures and their corresponding compositions.

3.1.1. Stage I – Exploratory Screening

Simulation results of all possible binary combinations of the ten refrigerants are shown in Fig 4, revealing consistent performance trends across all cases. As expected, Case III achieved a maximum COP of 6.50 with 70 % butane – 30 % hexane. This was followed by Case V and I, which reached COPs of 4.98 and 4.61 with pentane - heptane mixtures. Lastly, Case II and Case IV reached the highest COP with mixtures 60 % pentane – 40 % heptane and 50 % butane – 50 % hexane, respectively. Butane – hexane and pentane –heptane were therefore the best-performing hydrocarbon mixtures, consistently delivering the highest COP across four out of five load cases.

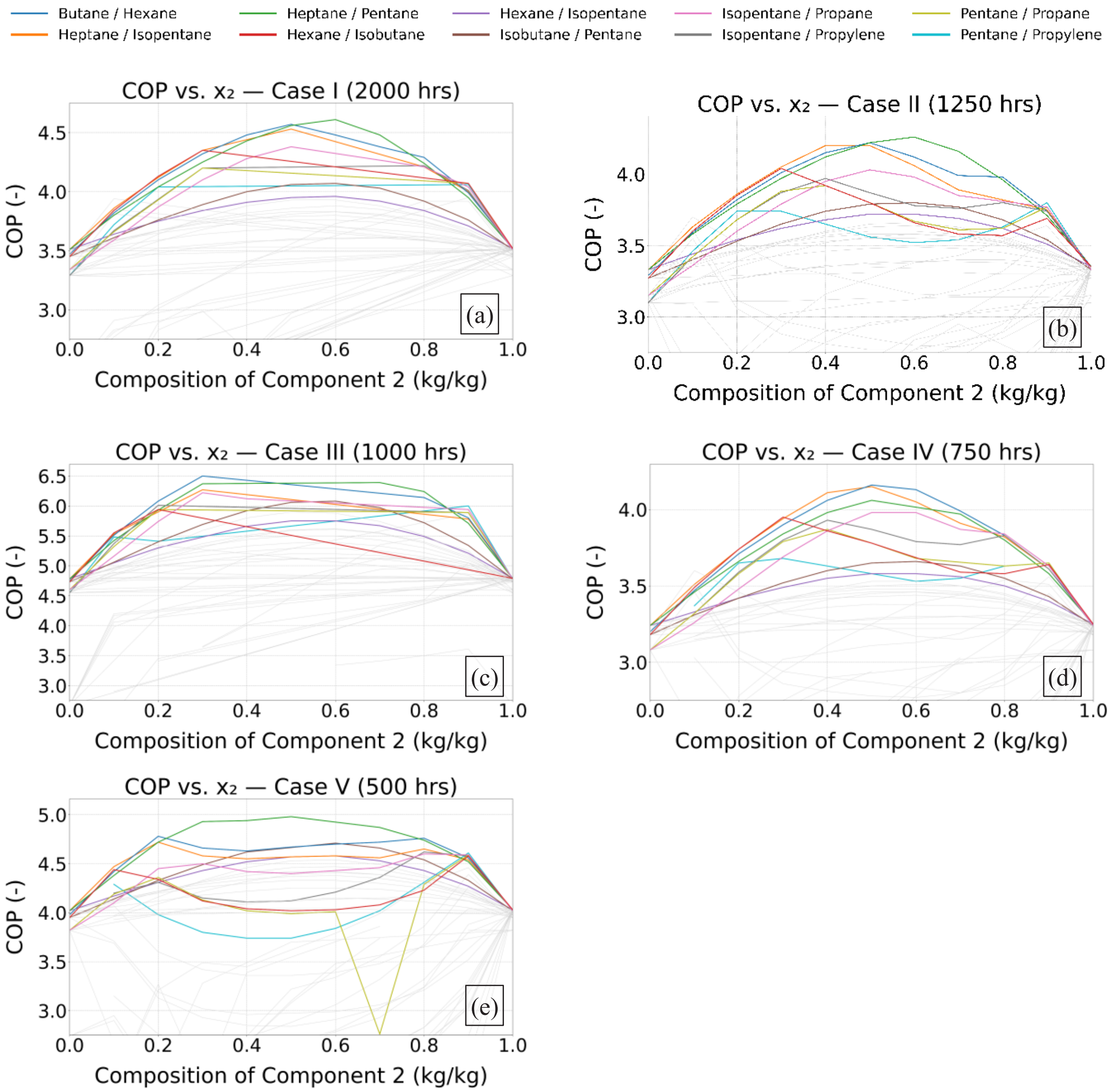

Figure 4. Performance of top 10 hydrocarbon mixtures for: (a) Case I, (b) Case II, (c) Case III, (d) Case IV, and (e) Case V.

3.1.2. Stage II – Refinement Screening

Following the initial evaluation of binary refrigerant mixtures based solely on thermodynamic performance, a second screening was carried out to incorporate practical constraints reflective of real-world system limitations. The filtered dataset was then refined with a higher resolution of composition steps, and exergy analysis was performed.

Table 4 summarizes the results of the refined screening. In Case I, where the source glide was minimal, 45 % propane -55 % isopentane emerged as the best-performing mixture, combining a high COP of 4.398 with low glide mismatches (π_{so} = 1.26 and π_{si} = 2.17). In Case II, the same mixture performed consistently well, again ranking first among all options with a COP of 4.04. Other noteworthy candidates in Case II include 60 % propylene – 40 % isopentane and 64 % propane – 36 % pentane, both exhibiting high COPs and reasonable glide indicators under increased source glide. In Case III, which had a favourable sink-source match and a smaller lift, significantly higher COPs were achieved. The 67 % propane – 33 % isopentane mixture delivered the highest COP recorded across all the cases with 6.325, with very well-matched glides, followed by 79 % propylene – 21 % isopentane and 82 % isobutane – 18 % hexane, all with good glide indicators and with COP of 6.059 and 6.052, respectively. In Case IV, the performance dropped slightly due to worse glide matching, but 44 % propane – 56 % isopentane and 60 % propylene – 40 % isopentane still showed good performance with moderate COPs around 4.0 and good glide match indicators. Lastly, Case V also yielded a high COP of 4.7 with the 21 % propylene – 79 % isopentane mixture. Generally, exergy analysis confirmed that the best results corresponded to mixtures with low π_{so} values, therefore good glide matching with the heat source temperature profile, even if the sink-side mismatch remains relatively larger. This suggests that aligning the refrigerant glide with the heat source has the strongest influence on overall cycle performance, which was consistent with Zühlsdorf et al. [16], who show that source-side matching governs efficiency because exergy losses are more significant at lower temperature levels.

Table 4. Top-performing HC mixtures for each case with COP, glide match indicators (π_{so} and π_{si}) and VHC

Medium	COP	π_{so} (–)	π_{si} (–)	p_{ev} (bar)	p_{co} (bar)	p_{co} / p_{ev} (–)	VHC (kJ/m³)
Case I							
45 % propane – 55 % isopentane	4.398	1.257	2.174	2.66	11.06	4.16	2383.9
64 % propane – 36 % pentane	4.293	1.550	2.199	3.58	14.23	3.97	3039.2
14 % ethane – 86 % isobutane	4.031	2.863	2.496	4.04	16.92	4.19	3321.4
8 % ethane – 92 % butane	4.020	3.317	2.795	2.26	11.36	5.03	2118.6
8 % ethane – 92 % butane	3.935	3.897	3.160	3.41	15.55	4.56	2950.9
Case II							
45 % propane – 55 % isopentane	4.044	1.302	2.389	2.63	12.23	4.65	2340.4
60 % propylene – 40 % isopentane	3.972	1.250	2.698	3.90	16.75	4.29	3254.6
64 % propane – 36 % pentane	3.969	1.506	2.402	3.57	15.63	4.38	3001.9
73 % propylene – 27 % pentane	3.774	2.146	2.941	4.57	19.97	4.37	3688.8
8 % ethane – 92 % butane	3.739	3.411	2.934	2.23	12.46	5.59	2075.5
Case III							
67 % propane – 33 % isopentane	6.325	1.670	1.530	5.64	13.74	2.44	4473.0
79 % propylene – 21 % isopentane	6.059	2.030	1.770	7.67	18.39	2.40	5759.0
82 % isobutane – 18 % hexane	6.052	2.440	1.800	2.34	6.87	2.94	2162.0
78 % propane – 22 % pentane	6.040	2.140	1.740	6.32	15.71	2.49	4900.0
12 % ethane – 88 % isobutane	5.979	1.970	2.020	5.43	14.14	2.60	4352.0
Case IV							
44 % propane – 56 % isopentane	4.020	1.241	1.801	2.58	12.20	4.73	2309.9
60 % propylene – 40 % isopentane	3.926	1.251	2.236	3.90	17.13	4.39	3266.7
64 % propane – 36 % pentane	3.898	1.506	2.115	3.57	16.20	4.54	3019.4
71 % propylene – 29 % pentane	3.694	2.156	2.693	4.31	19.95	4.63	3541.2
10 % ethane – 90 % butane	3.642	3.050	2.949	2.47	14.18	5.74	2271.8
Case V							
21 % propylene – 79 % isopentane	4.703	1.452	2.265	2.01	8.36	4.16	1920.8
21 % propane – 79 % isopentane	4.669	1.491	2.183	2.03	8.45	4.16	1920.7
86 % isobutane – 14 % hexane	4.581	2.395	2.274	2.79	10.97	3.93	2470.5
9 % ethane – 91 % butane	4.554	1.721	2.493	3.90	14.67	3.76	3325.8
43 % propylene – 57 % butane	4.544	1.855	2.967	5.54	19.17	3.46	4421.2

3.1.3. Stage III – Validation Screening

The final screening stage identified mixtures that combined high performance with stability across all operating cases. Each candidate was reassessed using a time-weighted COP reflecting annual load distribution, and a robustness check was performed by varying composition ±5 % to evaluate sensitivity to fractionation and composition shifts. Figure presents the top-performing mixtures for all five cases, where the coloured curves represent valid results from the first two screening stages, and grey areas correspond to the excluded or non-converged simulations.

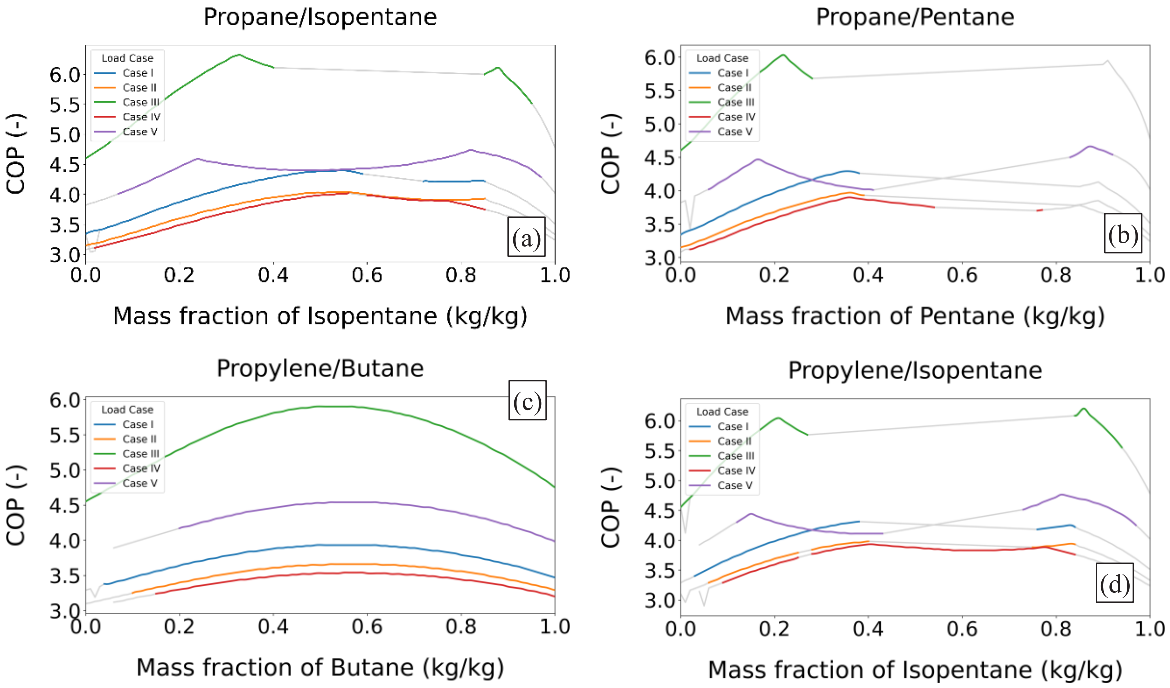

Figure 5. COP variation of the top-performing hydrocarbon mixtures across the five operational cases: (a) propane-isopentane, (b) propane-pentane, (c) propylene-butane, (d) propylene-isopentane.

From Figure , it is observed that the mixtures propane-isopentane, propane-pentane, and propylene-isopentane follow similar trends. The COP increased as the concentration of the second component increased, and it reached a maximum value when the first component was still dominant in the mixture. In all the mixtures, Case III always showed the steepest increase and highest peak in COP, especially in the case of propane-isopentane. On the contrary, the COP of propylene-butane steadily increased with butane concentration up to around 50 %, where it plateaus and started to decrease. By contrast, propylene-isopentane suffered from a fragmented dataset. Despite showing high COP values in Case III (around 6.1), the feasible composition range was broken into multiple segments, with large gaps in mid-composition ranges. Such high peaks observed in this, and other mixtures, highlight the strong potential of mixing refrigerants compared to pure fluids but also show the significant sensitivity of the COP to the mixture composition. Achieving and maintaining this optimal composition in real operation could be a practical challenge. The circulating composition of the mixture can easily deviate from the charged composition due to factors such as fractionation, leakages and mixing inconsistencies in the cycle. As shown in Figure , these small variations lead to changes in the performance of the mixture. To address this issue and ensure that performance gains are not overly sensitive to narrow composition ranges, a robustness criterion was introduced in the screening. Consequently, instead of selecting the optimal composition of the mixture solely based on the maximum COP achieved, a composition interval ± 5 % around the optimal point was used to define a robust composition zone. Moreover, a weighting factor was introduced corresponding to the number of hours attributed to each of the operating cases, with the purpose of considering their individual contribution to the annual performance of the system. Table 5 shows the results of the final analysis of the candidate refrigerants. The results demonstrate stable performance of the mixtures with limited sensitivity to composition changes. Propane-isopentane achieves the highest COP_{avg} (4.49) at the optimal composition of 66 % propane – 34 % isopentane, while maintaining high efficiency within ±5 % variation.

Table 5. Optimal composition and COP stability within ±5 % variation for top-performing mixtures.

Mixtures	$x_{2,opt}$ (kg/kg)	COP_{avg} at –5 % $x_{2,opt}$ (-)	COP_{avg} at $x_{2,opt}$ (-)	COP_{avg} at +5 % $x_{2,opt}$ (-)
propane-isopentane	0.34	4.384	4.491	4.621
propane-pentane	0.28	4.295	4.480	4.080
propylene-butane	0.61	4.255	4.351	4.255

Diving into the results for these mixtures applied to Case I, shown in Table 6, propane-isopentane, propane-pentane, and propylene-butane achieve COPs in the range of 3.93 to 4.18, also outperforming their pure fluid counterparts (COP 3.29 to 3.51) while maintaining significantly lower discharge temperatures than pure propane (131.5 ˚C) or propylene (140.3 ˚C).

Table 6. Performance comparison of the final selected refrigerants, showing COP, operating pressures, discharge temperature, and VHC for case I.

Working fluid(s)	COP (-)	p_{ev} (bar)	p_{co} (bar)	T_{disch} (°C)	VHC (kJ/m³)
Mixtures					
66 % propane – 34 % isopentane	4.18	3.82	15.29	119	3171
72 % propane – 28 % pentane	4.16	4.04	16.10	112	3332
39 % propylene – 61 % butane	3.93	3.07	14.49	119	2712
Pure fluids					
isopentane	3.51	0.41	4.28	118	497
propane	3.34	5.35	27.05	132	4194
pentane	3.51	0.29	3.43	121	376
propylene	3.29	6.57	31.53	140	4985
butane	3.47	1.20	9.29	123	1249

To visualize the performance differences between mixtures and pure fluids, T-Q diagrams were sketched using the example of 66 % propane – 34 % isopentane compared with pure propane. Figure 7 highlights the temperature glide of the mixture, which achieved a smoother alignment with both the source and sink temperature profiles. In the evaporator, the gradual slope of the mixture curve indicated reduced temperature mismatches and lower heat transfer irreversibility, while in the condenser, the improved overlap with the sink water line minimizes exergy losses. Conversely, pure propane exhibits a much steeper condensation profile (at constant temperature), leading to greater temperature mismatch and higher exergy destruction, ultimately resulting in a lower COP.

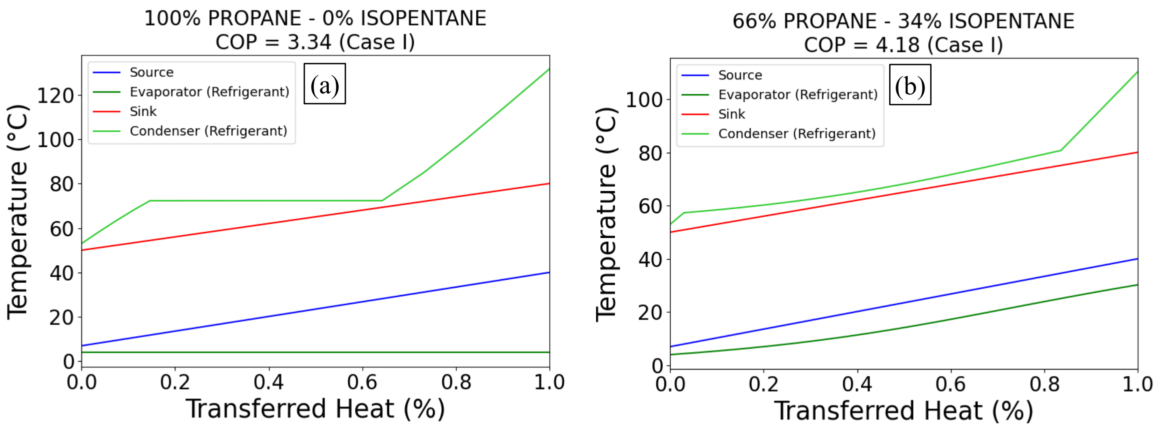

Figure 5. T-Q diagrams comparing mixture and pure fluid performance under Case I conditions: (a) pure propane and (b) 66% propane-34% isopentane

4. Discussion

While this study provides a structured and comparative framework for identifying high-performing zeotropic mixtures, some limitations can be acknowledged. Firstly, the present study focused exclusively on hydrocarbon mixtures**,** primarily due to their commercial availability and established safety protocols. This choice, although practical, potentially excluded other mixtures, particularly those containing low-GWP refrigerants, which might outperform hydrocarbons under certain conditions. Expanding the mixture set in future work could therefore yield a more comprehensive understanding of performance trade-offs among different refrigerant classes. Secondly, the compressor was modelled with a constant isentropic efficiency, independent of the fluid properties or pressure ratio. Such simplification might influence the practicality of the results to some extent. Furthermore, the system is simulated under steady state conditions, neglecting transient operations, and deviations of the circulating composition of the mixture from the charged composition, which can possibly occur in real systems using mixtures. These could alter the actual performance and robustness of the mixture in long-term operations. Finally, the study was carried out on five operating scenarios representative of a geothermal energy system. While it ensures consistency, it constrains the generalization of the results to other industrial applications operating under different thermal lifts and sink/source temperature profiles.

5. Conclusion

This study has demonstrated that hydrocarbon mixtures represent a technically and commercially promising pathway for enhancing the performance of district heating heat pumps with a geothermal heat source. Through the three-stage screening framework, mixtures such as propane-isopentane, propane-pentane, and propylene-butane consistently outperformed their pure fluid counterparts across multiple operating scenarios, achieving COP improvements of up to 25 %. These performance gains are attributed to the improved temperature glide matching between the refrigerant and the heat source and sink, which reduces exergy destruction in the heat exchangers. Overall, the results confirm that optimized hydrocarbon mixtures can deliver significant efficiency improvements without major system redesigns, supporting their potential as reliable, sustainable, and scalable working fluids for future heat pump applications.

Nomenclature

Abbreviations

GWP	Global Warming Potential
HCFO	Hydrochlorofluorooleins
HFC	Hydrofluorocarbon
HFO	Hydrofluoroolefin
HTHP	High temperature heat pump
IHX	Internal Heat Exchanger
ODP	Ozone depletion potential

Latin symbols

COP	Coefficient of performance, -
$\mathrm{COP_{avg}}$	Time-averaged coefficient of performance, -
$\dot{E}$	Exergy flow rate, W
f	Compressor heat loss factor, -
h_i	Specific enthalpy at state point *i*, kJ/kg
$\dot{Q}$	Heat flow rate, W
$\dot{m}$	Mass flow rate, kg/s
n	Discretization elements, -
p	Pressure, bar
t_i	Annual operating hours, h/year
T	Temperature, ˚C or K
$\bar{T}$	Thermodynamic average temperature, ˚C
$\dot{V}_i$	Volume flow rate at state point *i*, m^3/s
VHC	Volumetric heating capacity, kJ/m^3
x	Mixture composition, -
$\dot{W}$	Work rate, W

Greek Symbols

η_{is}	Isentropic efficiency compressor, -
η_{mech}	Mechanical efficiency compressor, -
π_{glide}	Glide matching indicator, -

Subscripts and Superscripts

avg	Average
boil	Boiling
comp	Compressor
cond	Condenser
crit	Critical
cold	Cold stream
d	Destruction
desup	Desuperheating
disch	Discharge
evap	Evaporator
f	Fuel
glide	Glide
hot	Hot stream
IHX	Internal Heat Exchanger
in	Inlet state
is	Isentropic
mech	Mechanical
opt	Optimal
out	Outlet state
p	Product
pinch	Pinch point temperature difference
sc	Subcooling
si	Sink stream
sh	Superheating
so	Source stream
0	Dead state

Acknowledgements

This research was partly funded by The Energy Technology Development and Demonstration Programme (EUDP) under the project title " HP2MIX - High Performance Heat Pumps with Zeotropic Mixtures", case no. 640242-533761.

References

[1] International Energy Agency (IEA), 2022. The future of heat pumps [www document]. https://www.iea.org/reports/the-future-of-heat-pumps (accessed 17 November 2025).
[2] Zühlsdorf B. High-performance heat pump systems: Enhancing performance and range of heat pump systems for industry and district heating. Kgs. Lyngby: Technical University of Denmark; 2019. 322 p. (DCAMM Special Report; No. S261).
[3] Zühlsdorf B, Jensen JK, Reinholdt LO, Elmegaard B. Comparison of zeotropic working fluid mixtures in different heat pump cycles. In: Proceedings of the 25th IIR International Congress of Refrigeration. International Institute of Refrigeration. 2019. p. 4673-4680. 1169. (Refrigeration Science and Technology, Vol. 2019-August). doi: 10.18462/iir.icr.2019.1166.
[4] Zhu T, Vieren E, Liang J, Thorsen JE, De Paepe M, Lecompte S et al. Booster heat pump with drop-in zeotropic mixtures applied in ultra-low temperature district heating system. Energy. 2024;305:132292. doi: 10.1016/j.energy.2024.132292
[5] Zühlsdorf B, Meesenburg W, Ommen TS, Thorsen JE, Markussen WB, Elmegaard B. Improving the performance of booster heat pumps using zeotropic mixtures. Energy. 2018;154:390-402. doi: 10.1016/j.energy.2018.04.137
[6] Abedini H, Vieren E, Demeester T, Beyne W, Lecompte S, Quoilin S, Arteconi A. A comprehensive analysis of binary mixtures as working fluid in high temperature heat pumps. Energy Convers. Manag. 2023;277:116652. doi: 10.1016/j.enconman.2022.116652.
[7] Zühlsdorf B, Bühler F, Mancini R, Cignitti S, Elmegaard B. High temperature heat pump integration using zeotropic working fluids for spray srying facilities. In: Proceedings of the 12th IEA Heat Pump Conference. Rotterdam; 2017.
[8] Guo H, Gong M, Qin X. Performance analysis of a modified subcritical zeotropic mixture recuperative high-temperature heat pump. Appl Energy. 2019;237:338-352. doi: 10.1016/j.apenergy.2018.12.094.
[9] Agrawal N, Patil S, Nanda P. Experimental studies of a domestic refrigerator using R290/R600a zeotropic blends. Energy Procedia. 2017;109:425-430. doi: 10.1016/j.egypro.2017.03.051.
[10] Zühlsdorf B, Jensen JK, Elmegaard B. Heat pump working fluid selection—economic and thermodynamic comparison of criteria and boundary conditions. Int J Refrig. 2019;98:500-513. doi: 10.1016/j.ijrefrig.2018.11.034.
[11] Zühlsdorf B, Elmegaard B, Jensen JK. Numerical models for the design and analysis of heat pumps with zeotropic mixtures [dataset]. Technical University of Denmark; 2018. doi:10.11583/DTU.6825443.v1.
[12] Python Software Foundation, Python, version 3.9.[software]. 2024.
[13] Lemmon EW, Huber ML, McLinden MO. NIST Standard Reference Database 23: Reference Fluid Thermodynamic and Transport Properties–REFPROP, Version 9.1. Gaithersburg (MD): National Institute of Standards and Technology; 2013 . Available from: https://www.nist.gov/publications/nist-standard-reference-database-23-reference-fluid-thermodynamic-and-transport (accessed 6 May 2025)
[14] Bell IH, Wronski J, Quoilin S, Lemort V. Pure and pseudo-pure fluid thermophysical property evaluation and the open-source thermophysical property library CoolProp. Ind Eng Chem Res. 2014;53:2498-2508. doi: 10.1021/ie4033999.
[15] Vieren E, Demeester T, Beyne W, Arteconi A, De Paepe M, Lecompte S. The thermodynamic potential of high-temperature transcritical heat pump cycles for industrial processes with large temperature glides. Appl Therm Eng. 2023;234:121197. doi: 10.1016/j.applthermaleng.2023.121197.
[16] Zühlsdorf B, Jensen JK, Cignitti S, Madsen C, Elmegaard B. Analysis of temperature glide matching of heat pumps with zeotropic working fluid mixtures for different temperature glides. Energy. 2018;153:650-660. doi:10.1016/j.energy.2018.04.048.
[17] Tsatsaronis G. Thermoeconomic analysis and optimization of energy systems. Prog Energy Combust Sci. 1993;19(3):227-257. doi: 10.1016/0360-1285(93)90016-8.